ORIGINAL ARTICLE ASIAN JOURNAL OF MEDICAL SCIENCES

Advanced multiparametric magnetic resonance imaging of intra-axial posterior fossa tumors

Sweta Swaika

Assistant Professor, Department of Radiodiagnosis, Gajra Raja Medical College, Gwalior, Madhya Pradesh, India

Submission: 22-06-2023 Revision: 02-10-2023 Publication: 01-11-2023

ABSTRACT

Background: For early treatment planning, it is required that accurate diagnosis of intra-axial posterior fossa tumors can be done. However, imaging diagnosis can be challenging due to analogous magnetic resonance imaging (MRI) features. **Aims and Objectives:** The aim of the study was to determine the accuracy of advanced MRI sequences such as diffusion-weighted imaging and magnetic resonance spectroscopy (MRS) in diagnosis of intra-axial posterior fossa masses in a tertiary care center. **Materials and Methods:** This was a retrospective observational study including 43 patients with posterior fossa intra-axial space-occupying tumors. Mean of minimum apparent diffusion coefficient (ADC) values (mean ADCmin) was derived in tumor, and normal white matter regions and ADC ratio was estimated. On MRS, choline/creatinine (Cho/Cr) and Cho/N-acetyl aspartate (NAA) ratios were noted. Receiver operating characteristic (ROC) curve was used to determine cut-off values for mean tumor ADCmin, ADC ratio, Cho/Cr ratio, and Cho/NAA ratio. **Results**: The most common tumor was medulloblastoma (MB) (30.23%), followed by metastasis (25.58%), pilocytic astrocytoma (16.28%), brainstem glioma (9.3%), hemangioblastoma (6.98%), glioneuronal tumor (6.98%), and ependymoma (4.65%). MBs showed lowest mean tumor ADCmin ($0.57 \pm 0.12 \times 10^{-3}$ mm^2/s) and ADC ratio (0.92 ± 0.18) and highest Cho/Cr ratio (8.26 ± 3.9) and Cho/NAA ratio (6.4 ± 1.83) with significant difference from the group of remaining tumors. ROC curve analysis revealed cutoff values of $\leq 0.71 \times 10^{-3}$mm^2/s for ADCmin; $\leq$ 1.02 for ADC ratio; >3.76 for Cho/Cr ratio, and >3.2 for Cho/NAA ratio for the differentiation of MBs from other tumors. **Conclusion:** The combined use of ADCmin values, ADC ratio, Cho/Cr ratio, and Cho/NAA ratio can help in better non-invasive analysis of similarly appearing intra-axial posterior fossa tumors.

Key words: Intra-axial posterior fossa tumors; Diffusion-weighted imaging; Apparent diffusion coefficient values; Magnetic resonance spectroscopy; Medulloblastoma

Access this article online

Website: http://nepjol.info/index.php/AJMS

DOI: 10.3126/ajms.v14i11.55977

E-ISSN: 2091-0576

P-ISSN: 2467-9100

INTRODUCTION

It is known that the inferior part of the cranial vault below the tentorium cerebelli and above the foramen magnum constitutes the posterior fossa comprising the cerebellum, fourth ventricle, and majority of brainstem (pons and medulla).[1] It is bounded by the clivus, bilateral petromastoid bones, and occipital bone forming a closed space.[1] Infratentorial masses are comparatively more common in children (more than 1 year of age) than adults.[2] Medulloblastoma (MB), pilocytic astrocytoma (PCA), ependymoma (EP), and brainstem glioma (BG) are the most frequently occurring posterior fossa neoplasms in children more than 4 years of age.[2,3] The most common intra-axial infratentorial tumor in adults is cerebellar metastasis.[2] The other neoplastic lesions occurring infratentorially are glioneuronal tumor, hemangioblastoma, schwannoma, meningioma, and atypical teratoid/rhabdoid tumor.[2]

Since posterior fossa has less intracranial dimensions, a small amount of mass effect on posterior fossa structures from neoplasms causes more pressure symptoms.[2] For early

Address for Correspondence:
Dr. Sweta Swaika, Assistant Professor, Department of Radiodiagnosis, Gajra Raja Medical College, Gwalior - 474 009, Madhya Pradesh, India.
Mobile: +91-8714294744. **E-mail:** swetaswaika@gmail.com

treatment planning, it is required that accurate diagnosis of tumor type can be done; however, diagnosis of posterior fossa masses can be challenging due to analogous magnetic resonance imaging (MRI) features.[4] Standard MRI sequences (T1-weighted (T1W), T2W, and post-contrast T1W images) are vital in evaluating the site, extension, and features but are not always adequate in grading and characterizing these masses.[2,5-7] Hence, there is a need for advanced MRI sequences. Diffusion-weighted imaging (DWI) with apparent diffusion coefficient values (ADC) has been found useful in differentiating high-grade from low-grade supratentorial astrocytomas[8] and posterior fossa solid–cystic masses in children.[2-7] Magnetic resonance spectroscopy (MRS) can measure *in vivo* metabolites in particular regions in humans[9] and is used clinically in brain tumors.[4,10]

Aims and objectives

The aim was to determine the accuracy of advanced MRI sequences (DWI and MRS) in the diagnosis of intra-axial posterior fossa masses in a tertiary care center.

MATERIALS AND METHODS

A retrospective observational study was conducted in the radiology department of a tertiary care hospital for a period of 2 years and 6 months (from July 2020 to December 2022). All patients with posterior fossa intra-axial space-occupying tumors who underwent MRI in radiology department were included in the study. Findings on DWI and MRS were noted in Microsoft Excel 2007 sheet. Imaging findings of all patients were further correlated with pathohistology (after surgery or biopsy) except for four cases of BG and nine cases of metastases which were diagnosed based on the clinical and MRI findings (BG has limitation of sampling/biopsy and is usually treated with radiotherapy and metastases usually have a history of primary malignancy). We excluded patients if they had infarct/hemorrhage in posterior fossa, traumatic injury, congenital malformation, non-neoplastic lesions (such as infection, demyelination, and abscess), considerable artifacts in MRI images, previously received surgical/chemotherapy/radiotherapy treatment, or had small-sized lesion (<10 mm). This study was performed after approval by the institutional review board (11/IEC-GRMC/2023). Informed consent was obtained from all the patients or guardians before MRI for using their images and clinical information for academic, educational, and publication purposes without revealing their identity. All images were evaluated by an experienced neuroradiologist without previous knowledge of clinical history and pathohistological diagnosis.

MRI was done using a 1.5 Tesla scanner (Ingenia, Philips Healthcare, Netherlands) with head coil in supine position. Routine MRI brain protocol for space-occupying lesions incorporated the following sequences: multiplanar T2W sequences, axial fluid-attenuated inversion recovery, axial T1-weighted sequence (T1W), susceptibility-weighted imaging (SWI), DWI, and MRS. Then, multiplanar post-contrast fat-saturated T1W sequence (with gadolinium-based contrast agent at bolus dose of 0.1 mmol/kg, not more than 20 mL) was acquired.

We obtained DWI with single-shot echo-planar spin-echo technique with 0, 500, and 1000 s/mm^2 b values for all slices and following parameters: TR/TE 4.1 s/89 ms, slice thickness 4.5 mm, interslice gap 1 mm, FOV 220 mm, matrix 184×109, flip angle 90°, and NSA 2. ADC maps are routinely obtained from DWI using b-value of 1000 s/mm^2, and a different workstation was used for the calculation of minimum ADC values (ADCmin) from tumor regions. We positioned three spherical regions-of-interest (ROI) each of 15–20 mm diameter, manually on ADC maps analogous to enhancing solid tumor region having lowest ADC values (not including necrotic, calcifications, microhemorrhages, and cystic areas). Similarly, ROIs were also placed in the normal-looking white matter of opposite parenchyma. We calculated mean of ADCmin values (measured in $\times 10^{-3}$ mm^2/s) from the ROIs for both tumor and normal white matter regions. We divided tumor mean ADCmin from normal white matter mean ADCmin to estimate ADC ratio.

For MRS, we used point-resolved spectroscopy technique with TR 2000 ms and long and short TE of 144 msec and 26 msec, respectively. We analyzed the metabolite peaks of N-acetyl aspartate (NAA), choline (Cho), creatine (Cr), and lipid-lactate and noted the Cho/Cr and Cho/NAA ratios for the lesions.

We used Statistical Package for the Social Sciences program version 20 of IBM (USA) for statistical analysis. We derived mean with standard deviation (SD) for numerical data and analyzed using independent samples *t*-test. Frequency and percentage were determined for age group distribution and gender and analyzed using the Chi-square test. Pair-wise comparison of age, mean ADCmin, mean ADC ratio, mean Cho/Cr, and Cho/NAA ratios was done between the different tumor types. Receiver operating characteristic (ROC) curve was used to determine cutoff values for mean tumor ADCmin, ADC ratio, Cho/Cr ratio, and Cho/NAA ratio for those tumor pairs who had statistically significant difference. $P<0.05$ was considered statistically significant.

RESULTS

In this study, 43 patients with intra-axial space-occupying posterior fossa tumor on conventional MRI were included with mean±SD age of 25.89±20.3 years (range:

2–70 years). The most common age group was ≤10 years (14, 32.56%), followed by 21–30 years (9, 20.93%), 11–20 years (6, 13.95%), 41–50 years (5, 11.62%), and 31–40 years, 51–60 years, and 61–70 years (3 each, 6.98%). There were 23 males (53.5%) and 20 females (46.5%) with no gender predominance (P=0.65). The mean±SD age in females was 27.6±21.5 years (range: 4–70 years) and mean age in males±SD was 24.4±19.6 years (range: 2–70 years) without significant difference (P=0.61). The most common tumor was MB (30.23%, Figure 1), followed by metastasis (25.58%), PCA (16.28%), BG (9.3%, Figure 2), hemangioblastoma (6.98%), glioneuronal tumor (6.98%), and EP (4.65%, Figure 3).

DWI and ADC maps were obtained in all tumors. MRS was available in 38 patients (88.4%) including 11 cases of MB, 9 cases of metastasis, 6 cases of PCA, 4 cases of BG, 3 cases each of hemangioblastoma and glioneuronal tumor, and 2 cases of EP. The parameters of all the tumors included in this study are mentioned in Table 1.

There was a significant difference in mean ADCmin and ADC ratio upon comparing MBs with all other tumors pair wise (Table 2). On pair-wise comparison of other tumors, significant difference in mean tumor ADCmin and ADC ratio of metastases with PCAs (P=0.0005 and P=0.0015, respectively) and glioneuronal tumors (P=0.0002 and P=0.0012, respectively) was found. On comparing PCAs with other tumors, there was a significant disparity in mean tumor ADCmin and ADC ratio with BGs (P=0.0143 and P=0.0123, respectively) and EPs (P=0.0213 and P=0.026, respectively). There was a significant difference in mean tumor ADCmin and ADC ratio between BGs and glioneuronal tumors (P=0.0047 and P=0.0017, respectively) and also between glioneuronal tumors and EPs (P=0.0052 and P=0.0039, respectively).

There was a significant disparity in mean Cho/NAA ratio of MBs on pair-wise comparison with all other tumors and in mean Cho/Cr ratio between MBs and all other tumors except metastases and glioneuronal tumors (Table 2). Furthermore, significant difference was noted in mean Cho/Cr ratio for metastases with PCAs and BGs (P=0.02 and P=0.04, respectively). There was noteworthy disparity in mean Cho/NAA ratio for metastasis with PCAs and hemangioblastomas (P=0.0054 and P=0.0228, respectively); for PCAs with glioneuronal tumors and EPs (P=0.0485 and P=0.0149, respectively); and for hemangioblastomas with EPs (P=0.023) (Table 2). The cut-off values for mean tumor ADCmin, ADC ratio, Cho/Cr ratio, and Cho/NAA ratio for tumor pairs having statistically significant difference are shown in Table 3.

The tumors were divided into two groups, first group comprised MBs and second group consisted of remaining tumors. On group-wise comparison, there was a significant difference in mean tumor ADCmin, ADC ratio, Cho/Cr ratio, and Cho/NAA ratio between the two groups (Table 4). Mean tumor ADCmin and ADC ratio were lower and mean Cho/Cr and Cho/NAA ratios were higher in MBs as compared to other tumor groups. ROC curve analysis was done for the differentiation of MBs from other tumors group. It revealed cutoff values of ≤0.71 $\times 10^{-3}$mm^2/s for ADCmin having 92.3% sensitivity, 100% specificity, and area under the curve (AUC)=0.987; ≤1.02 for ADC ratio having 84.6%

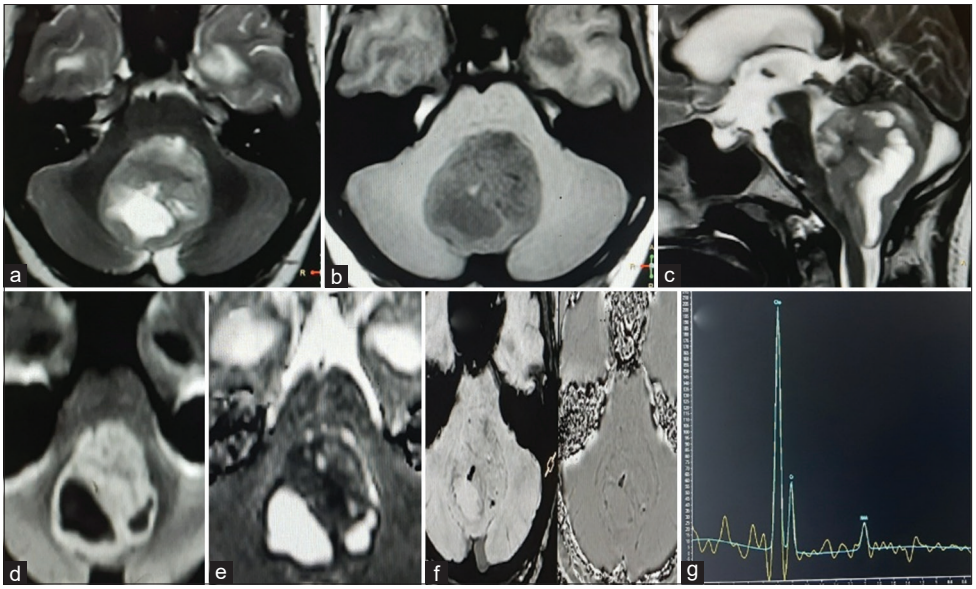

Figure 1: Medulloblastoma: Magnetic resonance imaging - (a) axial T2-weighted (T2W), (b) axial T1W, (c) sagittal T2W, (d) Diffusion-weighted imaging, (e) apparent diffusion coefficient, (f) susceptibility-weighted imaging (g) magnetic resonance spectroscopy

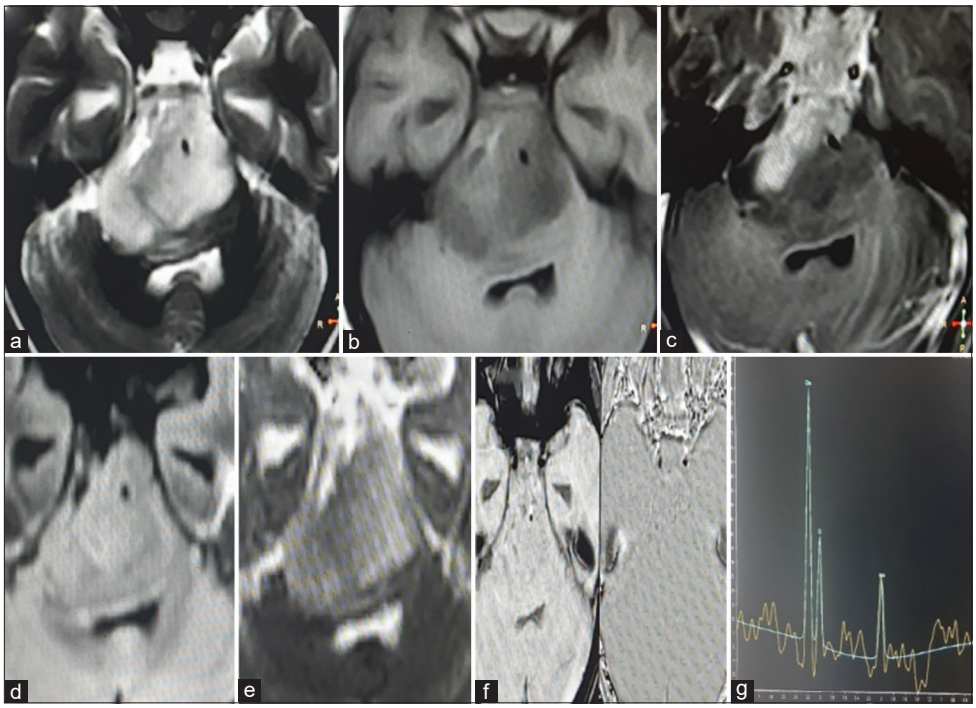

Figure 2: Brainstem glioma: Magnetic resonance imaging - (a) axial T2-weighted, (b) axial T1W, (c) axial post-contrast T1W, (d) Diffusion-weighted imaging, (e) apparent diffusion coefficient, (f) susceptibility-weighted imaging (g) magnetic resonance spectroscopy

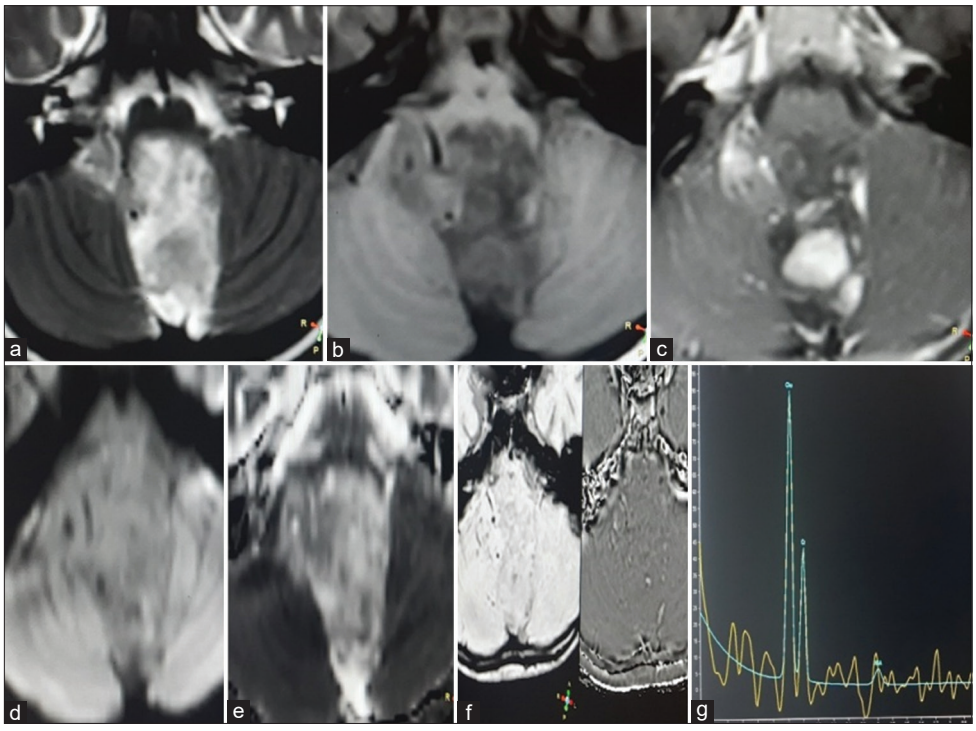

Figure 3: Ependymoma: Magnetic resonance imaging -(a) axial T2-weighted, (b) axial T1W, (c) axial post-contrast T1W, (d) Diffusion-weighted imaging, (e) apparent diffusion coefficient, (f) susceptibility-weighted imaging (g) magnetic resonance spectroscopy

sensitivity, 100% specificity, and AUC=0.977; >3.76 for Cho/Cr ratio having 100% sensitivity, 74.1% specificity, and AUC= 0.882; and >3.2 for Cho/NAA ratio having 100% sensitivity, 85.2% specificity, and AUC=0.98 (Table 4).

DISCUSSION

In this study, mean age was 25.89±20.3 years as the study included both pediatric and adult age groups. The mean age and median age in MBs were 11.07±7.8 years and 8 years,

Table 1: Study parameters of posterior fossa intra-axial tumors

Posterior fossa tumors	MB	Mets	PCA	BG	HB	GNT	EP
n (%)	13 (30.23%)	11 (25.58%)	7 (16.28%)	4 (9.3%)	3 (6.98%)	3 (6.98%)	2 (4.65%)
Age (years), mean±SD (range)	11.07±7.8 (2–25)	49.5±15.7 (18–70)	15.8±9.8 (5–30)	23.7±23.3 (4–55)	33.3±18.7 (22–55)	36.3±9.02 (27–45)	4.7±1.8 (3.5–6)
ADCmin, mean±SD (range)	0.57±0.12 (0.44–0.87)	1.02±0.19 (0.73–1.3)	1.51±0.29 (1.02–1.77)	1.01±0.2 (0.8–1.28)	1.33±0.23 (1.07–1.51)	1.62±0.09 (1.53–1.71)	0.86±0.15 (0.76–0.97)
ADC ratio, mean±SD (range)	0.92±0.18 (0.73–1.38)	1.58±0.37 (1.11–2.17)	2.34±0.47 (1.67–2.85)	1.53±0.27 (1.19–1.83)	2.07±0.39 (1.65–2.43)	2.51±0.04 (2.47–2.55)	1.33±0.27 (1.13–1.52)
Cho/Cr ratio, mean±SD (range)	8.26±3.9 (4.07–14.5)	5.8±3.2 (2.5–11.7)	2.3±0.87 (1.15–3.3)	1.99±0.62 (1.19–2.52)	1.94±0.24 (1.73–2.21)	3.63±1.73 (1.83–5.29)	1.95±0.7 (1.45–2.44)
Cho/NAA ratio, mean±SD (range)	6.4±1.83 (3.58–9.27)	2.95±1.15 (1.02–4.48)	1.23±0.61 (0.46–2.2)	1.59±0.91 (0.42–2.81)	1.06±0.52 (0.64–1.64)	2.8±1.45 (1.3–4.2)	2.78±0.18 (2.65–2.9)

MB: Medulloblastomas, Mets: Metastases, PCA: Pilocytic astrocytomas, BG: Brainstem gliomas, HB: Hemangioblastomas, GNT: Glioneuronal tumors, EP: Ependymomas, SD: Standard deviation, ADCmin: Minimum apparent diffusion coefficient ($\times 10^{-3}$ mm^2/s), ADC ratio: Apparent diffusion coefficient ratio, Cho/Cr=Choline/creatine ratio, NAA: N-acetyl aspartate

Table 2: Pair-wise comparison of parameters (P values) between posterior fossa tumors

Tumor comparison	Mean ADCmin	ADC ratio	Mean Cho/Cr	Mean Cho/NAA
MB and Mets	<0.0001	<0.0001	0.15	0.0001
MB and PCA	<0.0001	<0.0001	0.0024	<0.0001
MB and BG	0.0001	0.0001	0.008	0.0003
MB and HB	<0.0001	<0.0001	0.018	0.0004
MB and GNT	<0.0001	<0.0001	0.07	0.0089
MB and EP	0.0082	0.0133	0.049	0.0207
Mets and PCA	0.0005	0.0015	0.02	0.0054
Mets and BG	0.93	0.81	0.04	0.0621
Mets and HB	0.03	0.07	0.07	0.0228
Mets and GNT	0.0002	0.0012	0.29	0.86
Mets and EP	0.29	0.39	0.14	0.85
PCA and BG	0.0143	0.0123	0.55	0.47
PCA and HB	0.37	0.41	0.52	0.69
PCA and GNT	0.5495	0.56	0.1554	0.0485
PCA and EP	0.0213	0.026	0.6297	0.0149
BG and HB	0.105	0.08	0.9017	0.41
BG and GNT	0.0047	0.0017	0.1323	0.23
BG and EP	0.4107	0.441	0.946	0.16
HB and GNT	0.1117	0.124	0.1691	0.122
HB and EP	0.088	0.106	0.9821	0.023
GNT and EP	0.0052	0.0039	0.2991	0.98

MB: Medulloblastomas, Mets: Metastases, PCA: Pilocytic astrocytomas, BG: Brainstem gliomas, HB: Hemangioblastomas, GNT: Glioneuronal tumors, EP: Ependymomas, ADCmin: Minimum apparent diffusion coefficient, ADC ratio: Apparent diffusion coefficient ratio, Cho/Cr: Choline/creatine ratio, NAA: N-acetyl aspartate

respectively, as MBs are more common in the pediatric age group[2] but are also seen in adults.[1] The most common tumor was MB (30.23%) as it is the most common pediatric malignant posterior fossa tumor[2,11] and the most common age group was ≤10 years (32.56%). The second most common tumor was metastasis (25.58%) and was seen in the adult age group (18–70 years). Metastasis is the most common intra-axial posterior fossa tumor in adults,[1] also found in this study.

Mean tumor ADCmin and ADC ratio were lowest in MBs ($0.57\pm0.12\times10^{-3}$ mm^2/s and 0.92 ± 0.18, respectively). Similarly, low ADC values in MBs have been reported in the previous studies.[5,7,10,12] High-grade intracranial tumors have more intralesional cellularity and show hyperintensity in DWI images with lower ADC values,[5,7,13] which are seen in MBs[2] and high-grade gliomas.[8] The previous studies have shown usefulness of DWI with ADC maps in discriminating and grading intracranial tumors.[2,5,12-14] ADCmin is not as much influenced by inhomogeneity within the tumor[7] and areas of ADCmin coincide with the highest tumor grade;[6] hence, we used ADCmin for differentiating posterior fossa tumors. ROC curve analysis showed cutoff values of $\leq0.71\times10^{-3}$ mm^2/s for ADCmin and ≤1.02 for ADC ratio to distinguish MBs from other tumors. Pierce et al.[7] reported ADCmin cutoff value of <0.66 for discriminating MBs from other tumors, which is close to this study. Rumboldt et al.[14] reported an ADC cutoff value of 0.9×10^{-3} mm^2/s for MBs; however, they utilized overall mean tumor ADC and minimum ADC values was used in this study, thus cut-off ADC values are less in the present study.

Table 3: Cut-off values (with sensitivity and specificity) for mean tumor minimum apparent diffusion coefficient, apparent diffusion coefficient ratio, choline/creatine ratio and choline/N-acetyl aspartate ratio for tumor pairs with significant difference

Tumor comparison	ADCmin cut-off	ADC ratio cut-off	Mean Cho/Cr cut-off	Mean Cho/NAA cut-off
MB and Mets	≤0.71 (92.3%, 100%)	≤1.02 (84.6%, 100%)	-	>4.48 (81.8%, 100%)
MB and PCA	≤0.87 (100%, 100%)	≤1.38 (100%, 100%)	>3.3 (100%, 100%)	>2.2 (100%, 100%)
MB and BG	≤0.71 (92.3%, 100%)	≤1.16 (92.3%, 100%)	>2.52 (100%, 100%)	>2.81 (100%, 100%)
MB and HB	≤0.87 (100%, 100%)	≤1.38 (100%, 100%)	>2.21 (100%, 100%)	>1.64 (100%, 100%)
MB and GNT	≤0.87 (100%, 100%)	≤1.38 (100%, 100%)	-	>4.2 (81.8%, 100%)
MB and EP	≤0.71 (92.3%, 100%)	≤1.02 (84.6%, 100%)	>2.44 (100%, 100%)	>2.9 (100%, 100%)
Mets and PCA	≤1.3 (100%, 71.4%)	≤2.17 (100%, 71.4%)	>3.3 (66.7%, 100%)	>2.2 (77.8%, 100%)
Mets and BG	-	-	>2.52 (88.9%, 100%)	-
Mets and HB	≤1.3 (100%, 66.7%)	-	-	>1.64 (77.8%, 100%)
Mets and GNT	≤1.3 (100%, 100%)	≤2.17 (100%, 100%)	-	-
PCA and BG	>1.28 (71.4%, 100%)	>1.83 (85.7%, 100%)	-	-
PCA and GNT	-	-	-	≤2.2 (100%, 66.7%)
PCA and EP	>0.97 (100%, 100%)	>1.52 (100%, 100%)	-	≤2.2 (100%, 100%)
BG and GNT	≤1.28 (100%, 100%)	≤1.83 (100%, 100%)	-	-
HB and EP	-	-	-	≤1.64 (100%, 100%)
GNT and EP	>0.97 (100%, 100%)	>1.52 (100%, 100%)	-	-

MB: Medulloblastomas, Mets: Metastases, PCA: Pilocytic astrocytomas, BG: Brainstem gliomas, HB: Hemangioblastomas, GNT: Glioneuronal tumors, EP: Ependymomas, ADCmin: Minimum apparent diffusion coefficient, ADC ratio: Apparent diffusion coefficient ratio, Cho/Cr: Choline/creatine ratio, NAA: N-acetyl aspartate

Table 4: Comparison of parameters between medulloblastomas and other posterior fossa intra-axial tumors

Posterior fossa tumors	n (%)	ADCmin (mean±SD)	ADC ratio (mean±SD)	Cho/Cr (mean±SD)	Cho/NAA (mean±SD)
Medulloblastoma	13 (30.23)	0.57±0.12	0.92±0.18	8.26±3.9	6.4±1.83
Other tumors	30 (69.77)	1.21±0.33	1.88±0.53	3.49±2.5	2.12±1.2
P		<0.0001	<0.0001	0.0001	<0.0001
Cut-off values		≤0.71	≤1.02	>3.76	>3.2

ADCmin: Minimum apparent diffusion coefficient, ADC ratio: Apparent diffusion coefficient ratio, Cho/Cr: Choline/creatine ratio, NAA: N-acetyl aspartate, SD: Standard deviation

The mean ADCmin and ADC ratio of metastases were close to BGs as it included both low- and high-grade gliomas. Meyer et al.[15] reported mean ADC value of $0.98\pm0.32\times10^{-3}$ mm^2/s in brain metastases, almost similar to this study. There was a significant disparity in ADCmin on comparing metastases with hemangioblastomas (P=0.03). This is in contrast to Mustafa et al.,[5] who found no statistical difference in ADC values between them.

PCAs, hemangioblastomas, and glioneuronal tumors had relatively higher ADCmin and ADC ratio as compared to other tumors and had no significant difference between them as they are low-grade tumors.[2] The previous studies[5,6,14] have reported that PCAs have higher ADC value compared to high-grade tumors, analogous to this study. Significant difference in ADC ratio was found between PCAs and EPs with cutoff value of >1.52, similar to Koral et al.[16] and Gimi et al.,[17] who reported cutoff value of ≥1.8 and 1.7, respectively.

The peak age of incidence of EPs is 3–5 years,[2] and in this study also, it was found in children with a mean age of 4.7±1.8 years. EPs have been reported to have higher ADC value in comparison to MBs,[5,14] alike this study. This is due to the fact that EPs are moderately cellular with perivascular pseudorosettes and their cellularity is more in the anaplastic type.[5] Koral et al.[16] reported mean ADC and ADC ratio cutoff values of $<0.86\times10^{-3}$ mm^2/s and <1.2, respectively, for distinguishing EPs from MBs, close to this study. Gimi et al.[17] have reported ADC ratio cutoff value of 1.2 for correctly discriminating between EPs and MBs, comparable to this study. However, there was very small sample size of EPs in this study as it relatively less common than other tumors.

MRS informs about the biochemical features and metabolic inhomogeneity of tumors and adjacent brain parenchyma. High-grade tumors have increased choline, decreased NAA, and increase in Cho/Cr and Cho/NAA ratios.[4] MRS showed highest mean Cho/Cr ratio (8.26±3.9) and mean Cho/NAA ratio (6.4±1.83) in MBs which was significantly different when compared with other tumors having cutoff value of >3.76 (100% sensitivity and 74.1% specificity) and >3.2 (100% sensitivity and 85.2% specificity), respectively. Attia et al.,[4] reported a cut-off values of >3.5 (having 83% sensitivity and 78% specificity) for Cho/Cr ratio and >3.3 (having 92% sensitivity and 72% specificity) for Cho/NAA ratio for distinguishing high-grade masses from low-grade lesions. They found Cho/Cr ratio of 2.77–2.9 in low-grade EPs and 1.5–2 in BGs, comparable to this study.

Cuellar-Baena et al.[18] reported increased choline level and decreased NAA level in MBs relative to EPs and PCAs, analogous to this study. They showed that choline level of high-grade EPs was higher than that of PCAs and lower than MBs. Yuh et al.,[19] however, showed no significant difference in choline level between MBs and EPs, dissimilar to this study. Metastases showed high mean Cho/Cr ratio (mean 5.8±3.2) with significant difference with PCAs and BGs. Tsougos et al.[20] reported mean Cho/Cr and Cho/NAA ratios of 4.56±2.34 and 2.76±2.59, respectively, in intratumoral regions in brain metastasis, comparable to this study. However, it was not significantly dissimilar from intralesional part of glioblastomas. They found that peritumoral metabolite ratios could distinguish brain metastasis from glioblastomas. Attia et al.[4] and Panigrahy and Blüml[21] reported mild elevation of Cho/Cr and Cho/NAA ratios in PCAs similar to present study which occurs due to their low cellularity. The previous study have reported relatively lower Cho/Cr and Cho/NAA ratios in diffuse intrinsic pontine gliomas,[4] alike this study. Plaza et al.[22] reported that increase in choline on subsequent imaging in diffuse intrinsic pontine gliomas indicates increase in grade of tumor. The rest of the tumors did not show a significant disparity in Cho/Cr ratio among them. However, Cho/NAA ratio was significantly different on comparing PCAs with glioneuronal tumors and EPs; metastases with hemangioblastomas; and hemangioblastomas with EPs.

The previous studies have shown that there is additional advantage of a combination of advanced MRI sequences such as DWI using ADC values and MRS in accurately diagnosing and grading intracranial tumors.[23] Koob et al.[24] found that multiparametric MRI including DWI, MRS, and perfusion imaging are helpful in ascertaining grades (mainly Grades I and IV) and types of pediatric posterior fossa tumors (essentially for MBs and PCAs).

Limitations of the study

There was a small sample size with a less number of various posterior fossa lesions which remains the main limitation and entails further study with a larger number of masses. All images were evaluated by only one radiologist; hence, interobserver variability could not be ascertained. It was tried to select a representative group of different tumors, but this was a retrospective study and could have selection bias. There is a need for further prospective studies with larger sample size and also including perfusion MRI to better understand the usefulness of multiparametric MRI in patient treatment and outcome.

CONCLUSION

In conclusion, the combined use of advanced MRI techniques such as ADC values (ADCmin and ADC ratio) and MRS (Cho/Cr and Cho/NAA ratios) can help in better non-invasive analysis of similarly appearing intra-axial posterior fossa masses.

ACKNOWLEDGMENT

I hereby acknowledge all the patients, doctors, and staff for their help and cooperation during this study.

REFERENCES

1. Shih RY and Smirniotopoulos JG. Posterior fossa tumors in adult patients. Neuroimaging Clin N Am. 2016;26(4):493-510. https://doi.org/10.1016/j.nic.2016.06.003
2. Poretti A, Meoded A and Huisman TA. Neuroimaging of pediatric posterior fossa tumors including review of the literature. J Magn Reson Imaging. 2012;35(1):32-47. https://doi.org/10.1002/jmri.22722
3. Brandão LA and Poussaint TY. Posterior fossa tumors. Neuroimaging Clin N Am. 2017;27(1):1-37. https://doi.org/10.1016/j.nic.2016.08.001
4. Attia NM, Sayed SA, Riad KF and Korany GM. Magnetic resonance spectroscopy in pediatric brain tumors: How to make a more confident diagnosis. Egypt J Radiol Nucl Med. 2020;51(1):14. https://doi.org/10.1186/s43055-020-0135-3
5. Mustafa WF, Abbas M and Elsorougy L. Role of diffusion-weighted imaging in differentiation between posterior fossa brain tumors. Egypt J Neurol Psychiatry Neurosurg. 2020;56(1):39. https://doi.org/10.1186/s41983-019-0145-0
6. Al-Sharydah AM, Al-Arfaj HK, Al-Muhaish HS, Al-Suhaibani SS, Al-Aftan MS, Almedallah DK, et al. Can apparent diffusion coefficient values help distinguish between different types of pediatric brain tumors? Eur J Radiol Open. 2019;6:49-55. https://doi.org/10.1016/j.ejro.2018.12.004
7. Pierce T, Kranz PG, Roth C, Leong D, Wei P and Provenzale JM. Use of apparent diffusion coefficient values for diagnosis of pediatric posterior fossa tumors. Neuroradiol J. 2014;27(2):233-244. https://doi.org/10.15274/nrj-2014-10027
8. Raisi-Nafchi M, Faeghi F, Zali A, Haghighatkhah H and Jalal-Shokouhi J. Preoperative grading of astrocytic supratentorial brain tumors with diffusion-weighted magnetic resonance imaging and apparent diffusion coefficient. Iran J Radiol. 2016;13(3):e30426. https://doi.org/10.5812/iranjradiol.30426
9. Tognarelli JM, Dawood M, Shariff MI, Grover VP, Crossey MM, Cox IJ, et al. Magnetic resonance spectroscopy: Principles and techniques: Lessons for clinicians. J Clin Exp Hepatol. 2015;5(4):320-328. https://doi.org/10.1016/j.jceh.2015.10.006
10. Hellström J, Zapata RR, Libard S, Wikström J, Ortiz-Nieto F, Alafuzoff I, et al. The value of magnetic resonance spectroscopy as a supplement to MRI of the brain in a clinical setting. PLoS One. 2018;13(11):e0207336. https://doi.org/10.1371/journal.pone.0207336
11. Kerleroux B, Cottier JP, Janot K, Listrat A, Sirinelli D and Morel B. Posterior fossa tumors in children: Radiological tips and tricks in the age of genomic tumor classification and advance

MR technology. J Neuroradiol. 2020;47(1):46-53.
https://doi.org/10.1016/j.neurad.2019.08.002

12. Schneider JF, Confort-Gouny S, Viola A, Le Fur Y, Viout P, Bennathan M, et al. Multiparametric differentiation of posterior fossa tumors in children using diffusion-weighted imaging and short echo-time 1H-MR spectroscopy. J Magn Reson Imaging. 2007;26(6):1390-1398.
https://doi.org/10.1002/jmri.21185
13. Jaremko JL, Jans LB, Coleman LT and Ditchfield MR. Value and limitations of diffusion-weighted imaging in grading and diagnosis of pediatric posterior fossa tumors. AJNR Am J Neuroradiol. 2010;31(9):1613-1616.
https://doi.org/10.3174/ajnr.A2155
14. Rumboldt Z, Camacho DL, Lake D, Welsh CT and Castillo M. Apparent diffusion coefficients for differentiation of cerebellar tumors in children. AJNR Am J Neuroradiol. 2006;27(6):1362-1369.
15. Meyer HJ, Fiedler E, Kornhuber M, Spielmann RP and Surov A. Comparison of diffusion-weighted imaging findings in brain metastases of different origin. Clin Imaging. 2015;39(6):965-969.
https://doi.org/10.1016/j.clinimag.2015.06.015
16. Koral K, Alford R, Choudhury N, Mossa-Basha M, Gargan L, Gimi B, et al. Applicability of apparent diffusion coefficient ratios in preoperative diagnosis of common pediatric cerebellar tumors across two institutions. Neuroradiology. 2014;56(9):781-788.
https://doi.org/10.1007/s00234-014-1398-z
17. Gimi B, Cederberg K, Derinkuyu B, Gargan L, Koral KM, Bowers DC, et al. Utility of apparent diffusion coefficient ratios in distinguishing common pediatric cerebellar tumors. Acad Radiol. 2012;19(7):794-800.
https://doi.org/10.1016/j.acra.2012.03.004
18. Cuellar-Baena S, Morales JM, Martinetto H, Calvar J, Sevlever G, Castellano G, et al. Comparative metabolic profiling of paediatric ependymoma, medulloblastoma and pilocytic astrocytoma. Int J Mol Med. 2010;26(6):941-948.
https://doi.org/10.3892/ijmm_00000546
19. Yuh EL, Barkovich AJ and Gupta N. Imaging of ependymomas: MRI and CT. Childs Nerv Syst. 2009;25(10):1203-1213.
https://doi.org/10.1007/s00381-009-0878-7
20. Tsougos I, Svolos P, Kousi E, Fountas K, Theodorou K, Fezoulidis I, et al. Differentiation of glioblastoma multiforme from metastatic brain tumor using proton magnetic resonance spectroscopy, diffusion and perfusion metrics at 3 T. Cancer Imaging. 2012;12(3):423-436.
https://doi.org/10.1102/1470-7330.2012.0038
21. Panigrahy A and Blüml S. Neuroimaging of pediatric brain tumors: From basic to advanced magnetic resonance imaging (MRI). J Child Neurol. 2009;24(11):1343-1365.
https://doi.org/10.1177/0883073809342129
22. Plaza MJ, Borja MJ, Altman N and Saigal G. Conventional and advanced MRI features of pediatric intracranial tumors: Posterior fossa and supratellar tumors. AJR Am J Roentgenol. 2013;200(5):1115-1124.
https://doi.org/10.2214/AJR.12.9725
23. Darweesh AM, Badawy ME, Hamesa M and Saber N. Magnetic resonance spectroscopy and diffusion imaging in the evaluation of neoplastic brain lesions. Egypt J Radiol Nucl Med. 2014;45(2):485-493.
https://doi.org/10.1016/j.ejrnm.2014.03.002
24. Koob M, Girard N, Ghattas B, Fellah S, Confort-Gouny S, Figarella-Branger D, et al. The diagnostic accuracy of multiparametric MRI to determine pediatric brain tumor grades and types. J Neurooncol. 2016;127(2):345-353.
https://doi.org/10.1007/s11060-015-2042-4

Authors' Contributions:
SS – concept, design, data collection and analysis, statistical analysis, manuscript preparation, preparation of tables and figures, editing, revision, and manuscript submission.

Work attributed to:
Gajra Raja Medical College, Gwalior, Madhya Pradesh, India.

Orcid ID:
Sweta Swaika - https://orcid.org/0000-0001-8861-862X

Source of Support: Nil, **Conflicts of Interest:** None declared.